RESEARCH ARTICLE

INFECTION

Hyperglycemia drives intestinal barrier dysfunction and risk for enteric infection

Christoph A. Thaiss,[1] Maayan Levy,[1] Inna Grosheva,[2] Danping Zheng,[1] Eliran Soffer,[1] Eran Blacher,[1] Sofia Braverman,[1] Anouk C. Tengeler,[1] Oren Barak,[1,3] Maya Elazar,[1] Rotem Ben-Zeev,[1] Dana Lehavi-Regev,[1] Meirav N. Katz,[1] Meirav Pevsner-Fischer,[1] Arieh Gertler,[4] Zamir Halpern,[5,6,7] Alon Harmelin,[8] Suhail Aamar,[9] Patricia Serradas,[10] Alexandra Grosfeld,[10] Hagit Shapiro,[1] Benjamin Geiger,[2] Eran Elinav[1]*

Obesity, diabetes, and related manifestations are associated with an enhanced, but poorly understood, risk for mucosal infection and systemic inflammation. Here, we show in mouse models of obesity and diabetes that hyperglycemia drives intestinal barrier permeability, through GLUT2-dependent transcriptional reprogramming of intestinal epithelial cells and alteration of tight and adherence junction integrity. Consequently, hyperglycemia-mediated barrier disruption leads to systemic influx of microbial products and enhanced dissemination of enteric infection. Treatment of hyperglycemia, intestinal epithelial–specific GLUT2 deletion, or inhibition of glucose metabolism restores barrier function and bacterial containment. In humans, systemic influx of intestinal microbiome products correlates with individualized glycemic control, indicated by glycated hemoglobin levels. Together, our results mechanistically link hyperglycemia and intestinal barrier function with systemic infectious and inflammatory consequences of obesity and diabetes.

The obesity pandemic has reached alarming magnitudes, affecting more than 2 billion people worldwide and accounting for more than 3 million deaths per year (*1*). A poorly understood feature of the "metabolic syndrome" is its association with dysfunctions of the intestinal barrier, leading to enhanced permeability and translocation of microbial molecules to the intestinal lamina propria and systemic circulation (*2*). This influx of immune-stimulatory microbial ligands into the vasculature, in turn, has been suggested to underlie the chronic inflammatory processes that are frequently observed in obesity and its complications (*3*), while entry of pathogens and pathobionts through an impaired barrier leads to an enhanced risk of infection in obese and diabetic individuals (*4*, *5*), particularly at mucosal sites (*6*). However, the mechanistic basis for barrier dysfunction accompanying the metabolic syndrome remains poorly understood. Beyond metabolic disease, enhanced intestinal permeability has also been linked with systemic inflammation in a variety of conditions, including cancer (*7*), neurodegeneration (*8*), and aging (*9*). Thus, there is an urgent scientific need to better define the molecular and cellular orchestrators and disruptors of intestinal barrier function, to devise strategies to counteract the detrimental systemic consequences of gut barrier alterations.

Obesity is associated with, but not required for, intestinal barrier dysfunction

We began our investigation of the drivers of gastrointestinal barrier dysfunction in obesity by hypothesizing that the adipokine leptin, a major orchestrator of mammalian satiety, may act as an obesity-associated regulator of barrier integrity. Leptin deficiency and resistance to leptin signaling are strongly associated with morbid obesity in mice and humans, and both leptin deficiency and resistance were previously suggested to contribute to intestinal barrier dysfunction and susceptibility to enteric infection (*10*–*13*). We used a mouse model featuring genetic dysfunction of the leptin receptor (LepR), leading to hyperphagia and morbid obesity (*db/db*, fig. S1A). Indeed, we detected elevated amounts of microbial pattern recognition receptor (PRR) ligands at multiple systemic sites in leptin-unresponsive *db/db* mice (Fig. 1, A to C), indicative of enhanced influx of gut commensal-derived products. A similar phenomenon was observed in leptin-deficient mice (*ob/ob*, fig. S1, B and C). To gain insight into the molecular signatures accompanying barrier dysfunction under aberrant leptin signaling, we performed RNA sequencing of colonic tissue, obtained from *db/db* mice and their wild-type (WT) littermates under steady-state conditions. Leptin unresponsiveness was associated with global alterations of transcription (fig. S1D), with several hundred genes featuring differential expression between both groups (fig. S1E). Among the genes whose expression was most strongly abrogated in obese mice were members of the tight and adherence junction structures (fig. S1F), protein complexes that inhibit paracellular flux of intestinal molecules into the lamina propria (*14*). Consequently, tight junction integrity was compromised in *db/db* mice (Fig. 1, D and E), leading to enhanced influx of luminal molecules and electrical current measured across the epithelial layer (Fig. 1, F and G).

To determine the consequences of barrier dysfunction in leptin-resistant mice, we used the murine *Citrobacter rodentium* model simulating human enteropathogenic *Escherichia coli* infection (*15*). A bioluminescent variant of *C. rodentium* allowed us to noninvasively track infection in vivo (*16*). In WT mice, *C. rodentium* caused a self-limiting, mainly gut-contained infection (Fig. 1, H to L). In contrast, *db/db* mice did not clear the pathogen from their intestine (Fig. 1, H and I), in line with previous reports (*12*). Notably, *db/db* mice also showed a significantly enhanced bacterial attachment to the intestinal wall (fig. S1, G and H) and featured *C. rodentium* colonization at systemic sites (Fig. 1, J to L, and fig. S1I). Similar susceptibility to *C. rodentium* was noted for leptin-deficient *ob/ob* mice (fig. S1, J to N).

To understand which cell type was responsible for LepR-mediated protection from enteric infection, we generated bone marrow chimeras, in which WT and *db/db* mice were used as either recipients or donors of bone marrow transplanted into lethally irradiated mice. Exacerbated infection and systemic spread of *C. rodentium* was observed whenever the bone marrow recipient was LepR-deficient, regardless of the source of bone marrow (Fig. 1, M and N, and fig. S1O), indicating that the nonhematopoietic compartment mediated resistance against infection. LepR expression on nonhematopoietic cells has been reported in multiple tissues, including the gut, liver, and most prominently the nervous system (*17*). Mice lacking LepR in intestinal epithelial cells (Villin-Cre:LepR$^{fl/fl}$) or hepatocytes (Albumin-Cre:LepR$^{fl/fl}$) did not show any signs of enhanced susceptibility to *C. rodentium* infection (fig. S2, A to F), whereas mice with LepR deficiency specifically in the nervous system (Nestin-Cre:LepR$^{fl/fl}$) featured an exacerbated (fig. S2, G to I), yet highly variable (fig. S2, J to O), bacterial growth. To further explore the possibility of neuronal leptin signaling driving barrier dysfunction and risk of infection, we generated mice with a specific

[1]Department of Immunology, Weizmann Institute of Science, Rehovot, Israel. [2]Department of Molecular Cell Biology, Weizmann Institute of Science, Rehovot, Israel. [3]Department of Obstetrics and Gynecology, Kaplan Medical Center, Rehovot, affiliated with the Hebrew University and Hadassah School of Medicine, Jerusalem, Israel. [4]The Robert H. Smith Faculty of Agriculture, Food and Environment, The Hebrew University, Rehovot, Israel. [5]Sackler Faculty of Medicine, Tel Aviv Sourasky Medical Center, Tel Aviv, Israel. [6]Research Center for Digestive Tract and Liver Diseases, Tel Aviv Sourasky Medical Center, Tel Aviv, Israel. [7]Digestive Center, Tel Aviv Sourasky Medical Center, Tel Aviv, Israel. [8]Department of Veterinary Resources, Weizmann Institute of Science, Rehovot, Israel. [9]Department of Medicine, Hadassah–Hebrew University Hospital, Jerusalem, Israel. [10]INSERM Centre de Recherche des Cordeliers, Sorbonne Université, Sorbonne Cités, UPD Univ. Paris 05, CNRS, IHU ICAN, Paris, France.
***Corresponding author. Email: eran.elinav@weizmann.ac.il**

deletion of LepR in the paraventricular hypothalamus (Sim1-Cre:LepR$^{fl/fl}$), in the ventromedial hypothalamus (SF1-Cre:LepR$^{fl/fl}$), in cholinergic neurons (ChAT-Cre:LepR$^{fl/fl}$), and in the arcuate nucleus of the hypothalamus (POMC-Cre:LepR$^{fl/fl}$ and AgRP-Cre:LepR$^{fl/fl}$) and infected them with *C. rodentium*. However, none of these mice showed enhanced susceptibility to pathogenic invasion when compared to littermate controls (fig. S3, A to O). Collectively, these results suggested that leptin deficiency per se might not provide a sufficient explanation to barrier dysfunction and enhanced risk of enteric infection.

A feature common to all leptin- and LepR-deficient mice exhibiting an impaired barrier function and enhanced *C. rodentium* dissemination in our studies (*db/db, ob/ob* and Nestin-Cre:LepR$^{fl/fl}$) was their tendency to develop obesity. We therefore hypothesized that an obesity-related factor distinct from leptin signaling may predispose these mice to impaired barrier function and exacerbated intestinal infection. Thus, to complement the above genetic models of obesity, we fed WT mice a high-fat diet (HFD) to induce weight gain (fig. S4A). Similarly to obese leptin- and LepR-deficient mice, HFD-fed obese mice showed elevated steady-state systemic PRR ligand influx (Fig. 2A), as well as exacerbated *C. rodentium* infection and systemic dissemination (Fig. 2, B to E, and fig. S4B). To further test whether obesity is the major driver for barrier dysfunction and impaired *C. rodentium* containment in LepR-deficient mice, we performed paired-feeding experiments, in which the food access for *db/db* mice was restricted to the amount consumed by their WT littermates, thereby equalizing body weight between both groups (Fig. 2F). Surprisingly, even after weight reduction to control levels, lean *db/db* mice were still unable to cope with *C. rodentium* infection (Fig. 2, G and H), ruling out that obesity per se was directly driving barrier dysfunction and risk for enteric infection in these mice. The lack of a direct causal relationship between obesity and barrier dysfunction was further supported by experiments using a chemical inhibitor of leptin signaling (*18*), which rendered WT mice susceptible to exacerbated infection and systemic bacterial spread even before the onset of marked obesity (Fig. 2, I to L, and fig. S4, C to F). Together, these data indicated that neither leptin signaling nor obesity per se sufficiently explain the severity of barrier dysfunction and systemic enteric infection in mice with the metabolic syndrome.

In search of a unifying explanation for the above results in multiple mouse models of genetic and acquired obesity and leptin deficiency, we investigated other common features of the metabolic syndrome that could potentially contribute to barrier dysfunction. One such manifestation

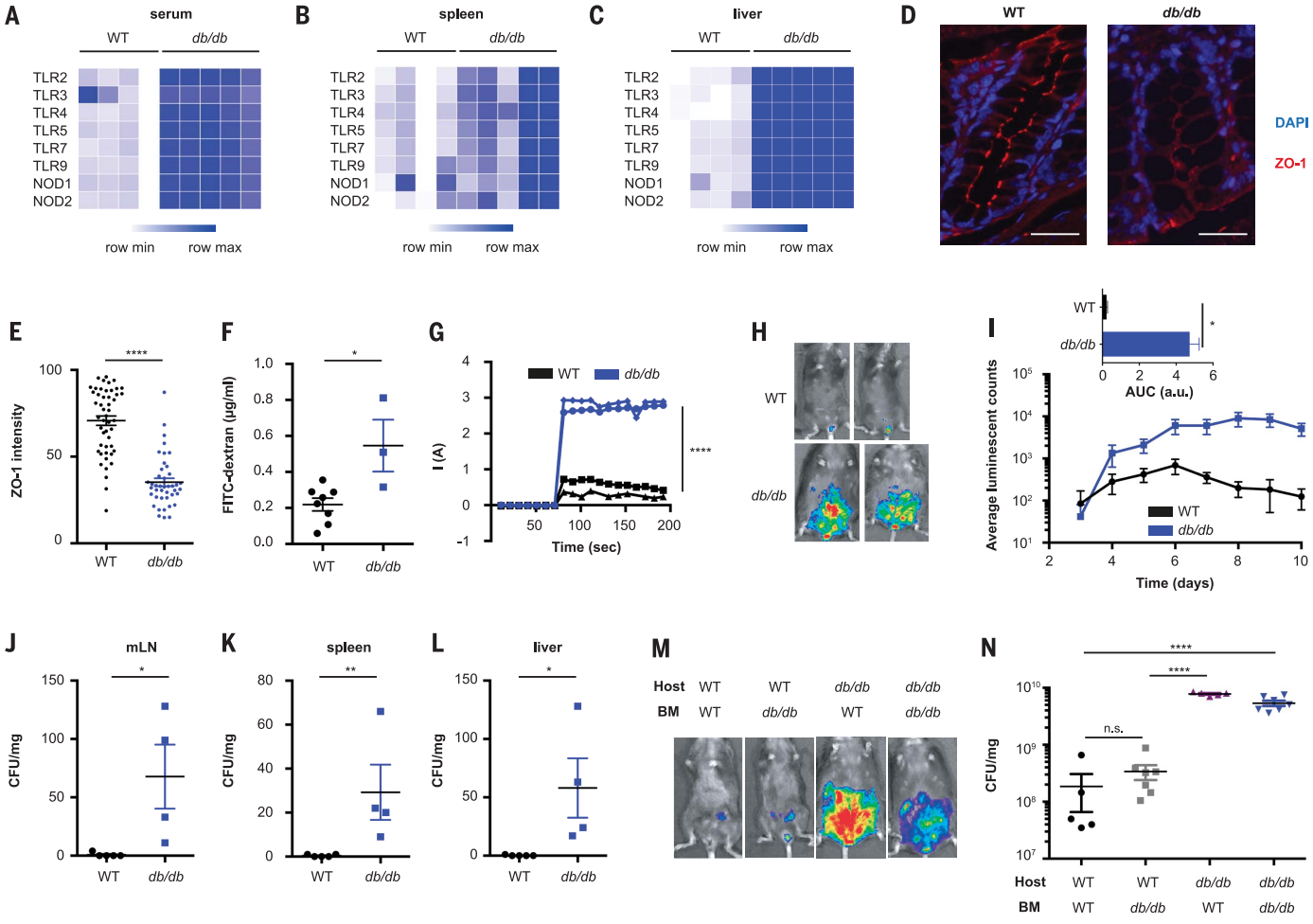

Fig. 1. Obesity is associated with intestinal barrier dysfunction and enteric infection. (**A** to **C**) PRR stimulation by sera (A) and splenic (B) and hepatic extracts (C) from *db/db* mice and WT littermates. (**D** and **E**) ZO-1 staining (D) and quantification (E) of colonic sections from *db/db* mice and WT littermates. Scale bars, 100 μm. (**F**) FITC (fluorescein isothiocyanate)–dextran recovered from the serum of *db/db* mice and WT littermates after oral gavage. (**G**) Ussing chamber recording of colons from *db/db* mice and controls. (**H** to **L**) Abdominal luminescence (H and I) and colony-forming units (CFUs) recovered from mesenteric lymph nodes (J), spleens (K), and livers (L) from *db/db* mice infected with *C. rodentium*. (**M** and **N**) Total abdominal luminescence (M) and epithelial-adherent colonies (N) of *C. rodentium* in bone marrow chimeras of *db/db* and WT mice. All data represent at least two independent experiments. Means ± SEM are plotted. *P < 0.05, **P < 0.01, ****P < 0.0001 by analysis of variance (ANOVA) (N) or Mann-Whitney U test (all other panels). ns, not significant.

of the metabolic syndrome, typically accompanying obesity and potentially contributing to barrier dysfunction, is glucose intolerance and resultant hyperglycemia. Notably, all mice featuring marked susceptibility *C. rodentium* infection, including obese *db/db*, pair-fed lean *db/db* mice, Nestin-Cre:LepR$^{fl/fl}$ mice, mice fed a HFD, and mice treated with leptin antagonist, showed elevated blood glucose concentrations (Fig. 2, M to O, and fig. S4, G and H). In contrast, all mouse groups and models that did not develop enhanced *C. rodentium* susceptibility (Villin-Cre:LepR$^{fl/fl}$, Albumin-Cre:LepR$^{fl/fl}$, Sim1-Cre:LepR$^{fl/fl}$, SF1-Cre:LepR$^{fl/fl}$, ChAT-Cre:LepR$^{fl/fl}$, POMC-Cre:LepR$^{fl/fl}$, and AgRP-Cre:LepR$^{fl/fl}$, as well as those Nestin-Cre:LepR$^{fl/fl}$ mice that did not feature a tendency for severe infection) collectively showed normoglycemic levels (fig. S4, I and J). Together, these results suggested that hyperglycemia, rather than obesity or alterations in leptin signaling, may predispose to barrier dysfunction leading to enhanced enteric infection in the setup of the metabolic syndrome in mice.

Hyperglycemia drives intestinal barrier disruption

To test whether elevated glucose concentrations were causally involved in host defense against intestinal infection, we induced hyperglycemia in the absence of obesity in a mouse model of type 1 diabetes mellitus through administration of streptozotocin [STZ (*19*), fig. S5A]. Indeed, STZ-treated mice developed severe *C. rodentium* infection and systemic translocation, accompanied by enhanced bacterial growth, epithelial adherence, and systemic spread (Fig. 3, A to E). STZ treatment also resulted in dysfunction of intestinal epithelial adherence junctions under steady-state conditions (Fig. 3, F and G), coupled with systemic dissemination of microbial products (fig. S5, B and C), and enhanced transepithelial flux (Fig. 3, H and I).

Oral antibiotic treatment prevented the detection of bacterial products at systemic sites in STZ-treated mice (Fig. 3, J to L), demonstrating that the intestinal microbiota was the probable source of disseminated microbial molecules. In contrast to the load of bacterial products at distal organs (fig. S5D), the microbial load in the intestinal lumen was unaffected by hyperglycemia (fig. S5E). We next sought to test the possibility that barrier dysfunction in STZ-treated mice was mediated by compositional microbiota alterations. Indeed, 16*S* ribosomal DNA (rDNA) sequencing revealed a taxonomic change in the configuration of the intestinal microbiota of hyperglycemic mice, which was corrected by insulin treatment and resultant normalization of serum glucose concentrations (fig. S6, A to D). However, these compositional microbial changes did not seem to play a critical role in glucose-mediated barrier dysfunction, as microbiota transfer from STZ-treated

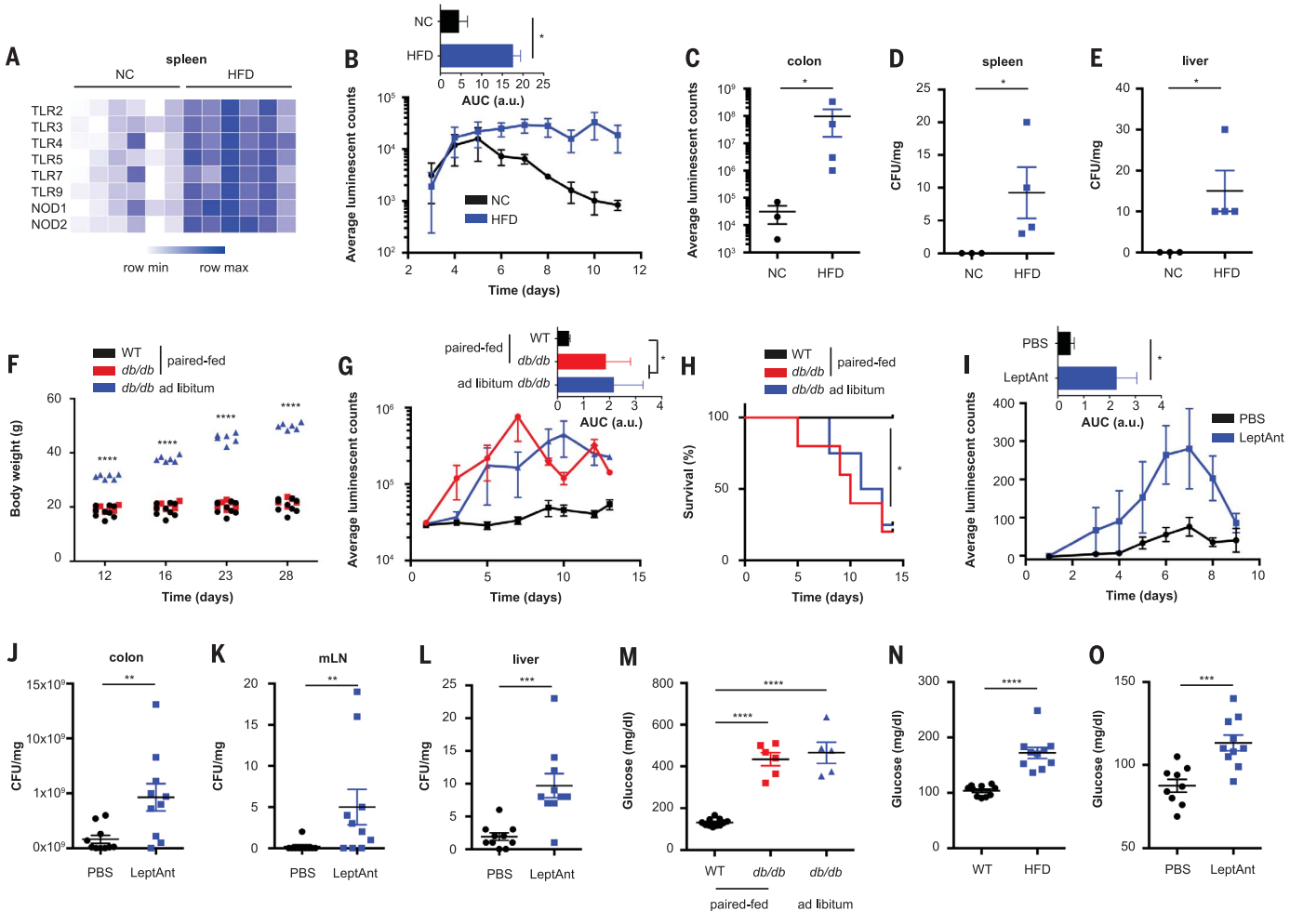

Fig. 2. Obesity does not suffice to explain susceptibility to enteric infection. (**A**) PRR stimulation by splenic extracts from mice fed a high-fat diet (HFD). (**B** to **E**) Abdominal luminescence (B) and CFUs recovered from colonic tissue (C), spleens (D), and livers (E) of HFD-fed mice infected with luminescent *C. rodentium*. (**F** to **H**) Body weight (F), *C. rodentium* luminescence (G), and *C. rodentium*-induced mortality (H) in paired-fed *db/db* mice and controls. (**I** to **L**) Total abdominal luminescence signals (I) and live CFUs recovered from colonic tissue (J), mesenteric lymph nodes, (K) and livers (L) from leptin antagonist (LeptAnt)-treated mice infected with bioluminescent *C. rodentium*. (**M** to **O**) Blood glucose concentrations in paired-fed *db/db* mice (M), HFD-fed mice (N), and LeptAnt-treated mice (O). All data represent at least two independent experiments. Means ± SEM are plotted. **P* < 0.05, ***P* < 0.01, ****P* < 0.001, *****P* < 0.0001 by ANOVA (F and M) or Mann-Whitney *U* test (all other panels).

donors and controls to normoglycemic germ-free mice neither induced dissemination of bacterial products to systemic sites (fig. S6E) nor increased susceptibility to *C. rodentium* infection (fig. S6, F to J). These data indicate that although the commensal microbiota serves as the reservoir of microbial molecules that translocate to the systemic circulation upon disruption of the intestinal barrier, compositional microbiota alterations arising under hyperglycemic conditions do not directly affect barrier integrity.

To corroborate the specificity of hyperglycemia as a driver of susceptibility to intestinal infection, we used hyperglycemic *Akita* mice (fig. S7A), an STZ-independent model of type I diabetes mellitus that harbors a spontaneous mutation in the gene encoding insulin 2 (*20*). As in STZ-treated mice, we observed in this model elevated *C. rodentium* growth and pathogenic translocation to systemic tissues (Fig. 3, M and N, and fig. S7, B and C). To further validate the specific impact of hyperglycemia as a driver of the barrier dysfunction phenotype, we administered 0.25 U per day of insulin to STZ-treated mice via hyperosmotic pumps for 4 weeks, which restored normoglycemic levels (fig. S7D). Treatment with insulin also prevented the loss of adherence junction integrity (Fig. 4A and fig. S7E), systemic dissemination of microbial products (Fig. 4B), and enhanced *C. rodentium* growth and pathogenic translocation (Fig. 4, C and D). Together, these experiments establish hyperglycemia as a direct and specific cause for intestinal barrier dysfunction and susceptibility to enteric infection.

Hyperglycemia reprograms intestinal epithelial cells

To determine whether glucose acted directly on intestinal epithelial cells to affect barrier function, we used an in vitro system of cultured intestinal epithelial (Caco-2) cells exposed to different concentrations of glucose in the culture medium. We assessed tight junction integrity through automated high-throughput analysis of ZO-1 staining patterns. Indeed, glucose induced barrier alterations in a dose- and time-dependent manner, manifesting visually as increased tortuosity and altered appearance of cell-cell junctions (Fig. 4, E to H). To investigate the mechanisms by which elevated blood glucose concentrations compromise intestinal epithelial cell function in vivo, we performed RNA sequencing of purified intestinal epithelial cells from STZ-treated mice and controls. Global reprogramming of the epithelial transcriptome was detected in hyperglycemic mice (Fig. 4I), in which more than 1000 genes were differentially expressed compared to vehicle-treated controls (Fig. 4J). These genes were predominantly involved in metabolic pathways, and specifically in N-glycan biosynthesis and pentose-glucuronate interconversion (Fig. 4K), two intracellular functions critically involved in the maintenance of epithelial barrier function (*21*–*29*). For example, hyperglycemia affected the entire pathway of protein N-glycosylation by provoking marked downregulation of central genes (Fig. 4L and fig. S8). In contrast, epithelial proliferation or cell death were not affected by STZ treatment (fig. S9, A to D).

In addition to the above epithelial changes, hyperglycemia modestly affected the intestinal

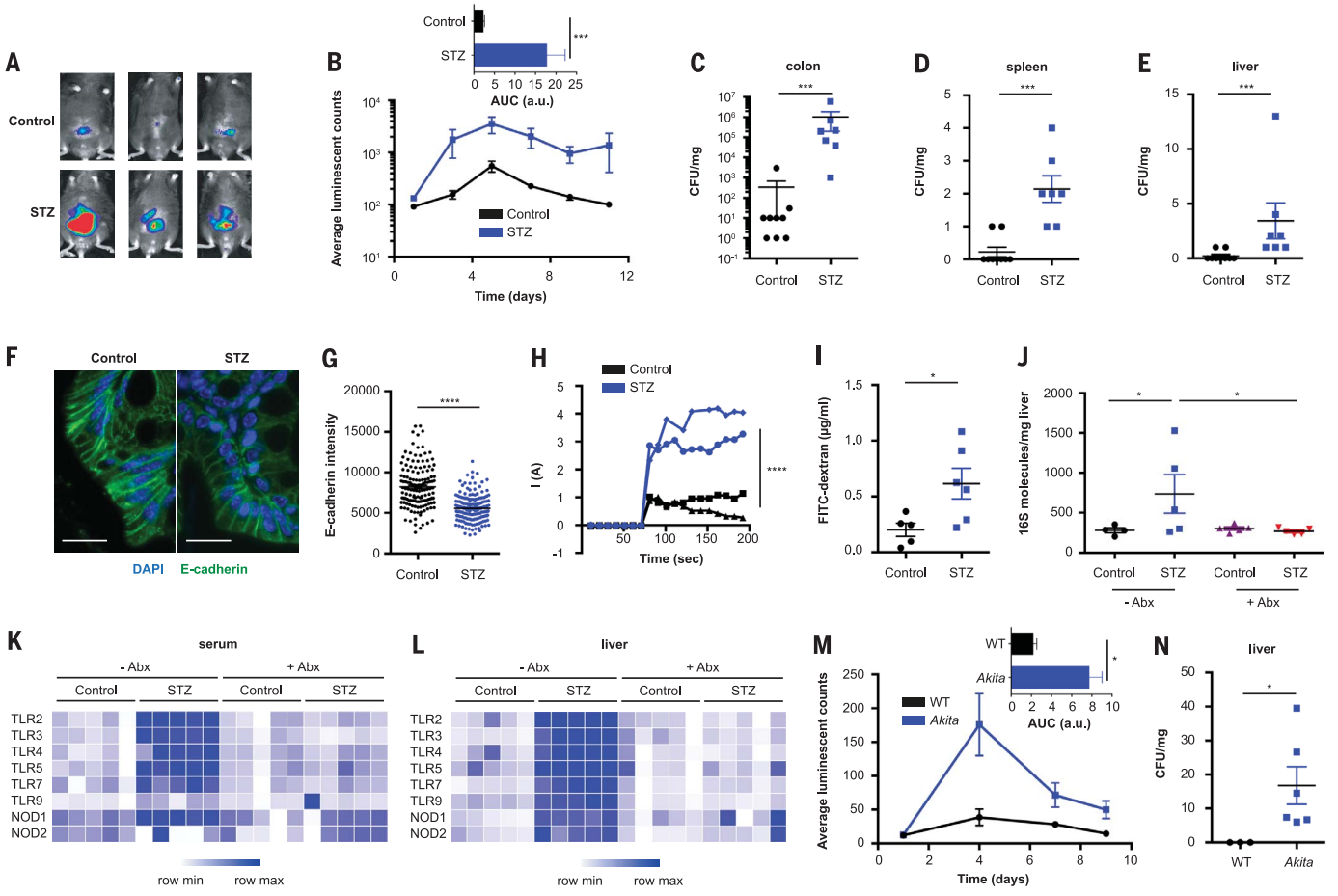

Fig. 3. Hyperglycemia causes susceptibility to enteric infection. (**A** to **E**) Abdominal luminescence (A and B) and CFUs recovered from colonic tissue (C), spleens (D), and livers (E) from STZ-treated mice infected with bioluminescent *C. rodentium*. (**F** and **G**) E-cadherin staining (F) and quantification (G) of colons from STZ-treated mice and controls. Scale bars, 25 µm. (**H**) Ussing chamber recordings from colons of STZ-treated mice and controls. (**I**) FITC-dextran recovered from the serum of STZ-treated mice after oral gavage. (**J**) Detection of 16*S* rDNA in livers of STZ- and Abx-treated mice. (**K** and **L**) PRR stimulation by sera (K) and hepatic extracts (L) from STZ-treated mice and controls, with or without antibiotic (Abx) treatment. (**M** and **N**) Abdominal luminescence (M) and hepatic CFUs (N) from *C. rodentium*–infected *Akita* mice. All data represent at least two independent experiments. Means ± SEM are plotted. *$P < 0.05$, ***$P < 0.001$, ****$P < 0.0001$ by ANOVA (J) or Mann-Whitney *U* test (all other panels).

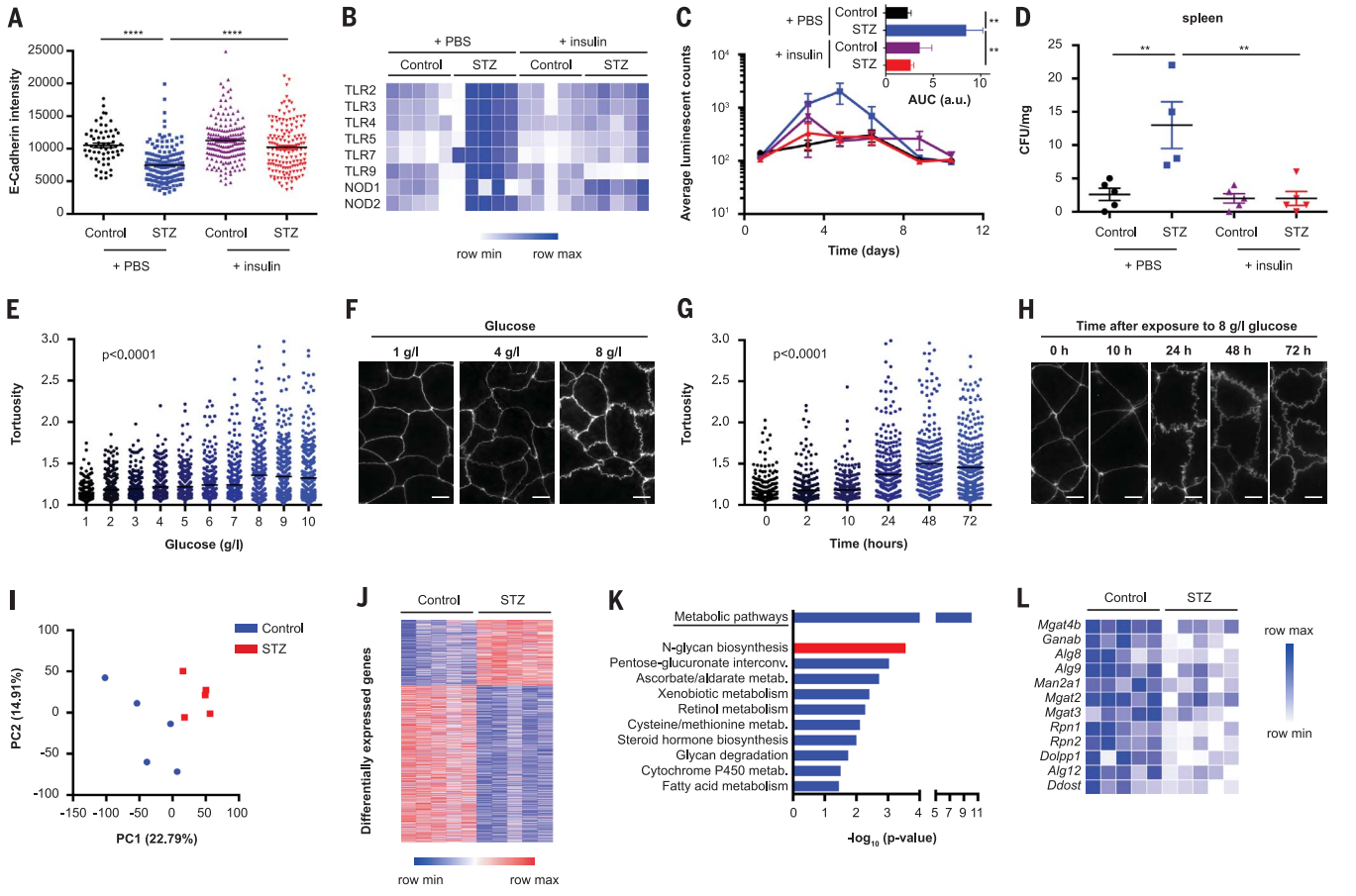

Fig. 4. Hyperglycemia alters intestinal epithelial cell function. (**A** and **B**) Colonic E-cadherin intensity (A) and PRR ligand stimulation by sera (B) from STZ-treated mice and controls, with or without insulin administration. (**C** and **D**) Abdominal luminescence (C) and CFUs recovered from the spleen (D) of STZ- and insulin-treated mice after *C. rodentium* infection. (**E** to **H**) Quantification of barrier tortuosity (E and G) and representative ZO-1 staining (F and H) of Caco-2 cells treated with different concentrations and exposure times of glucose. Scale bars, 10 μm. (**I** to **K**) Principal component analysis (I), heatmap (J), and pathway annotation (K) of differentially expressed genes in the epithelium of STZ-treated mice and controls. (**L**) Differentially expressed genes contributing to N-glycan biosynthesis. All data represent at least two independent experiments. Means ± SEM are plotted. $^{**}P < 0.01$, $^{****}P < 0.001$ by ANOVA.

and splenic immune system, specifically by causing an increased representation of myeloid cells (fig. S10, A to J), in line with previous reports (*30*). However, STZ treatment did not provoke an overt inflammatory state in the intestine (fig. S11, A to E). In particular, cytokines involved in interleukin-22 (IL-22)–mediated barrier function and host defense, which has been implicated in the susceptibility of obese mice to infection (*12*), were unaltered, as was the epithelial transcriptional response to IL-22 (fig. S11F). Indeed, hyperglycemia and IL-22 appeared to have additive effects in mediating host defense against *C. rodentium*, because STZ-treated IL-22–deficient mice featured accelerated bacterial growth and mortality when compared to IL-22–deficient controls (fig. S11, G and H). We further compared the involvement of epithelial and immune cells in host defense against another gastrointestinal pathogen, *Salmonella* Typhimurium. STZ-treated mice orally infected with *Salmonella* showed enhanced systemic colonization, whereas intestinal luminal growth was comparable to that of vehicle-treated controls (fig. S12, A to E). In contrast to this marked susceptibility of STZ-treated mice to oral *Salmonella* Typhimurium infection, susceptibility of these mice to systemic infection was only apparent in the liver (fig. S12, F to H). Notably, systemic infection with *Salmonella* caused enhanced intestinal colonization in STZ-treated mice, potentially indicative of retrograde spread of bacteria across a compromised barrier (fig. S12, I and J).

Epithelial reprogramming by hyperglycemia involves glucose metabolism and GLUT2

We next assessed whether epithelial glucose metabolism was involved in the transcriptional reprogramming of STZ-treated mice. Isolated intestinal epithelial cells from hyperglycemic mice featured elevated amounts of metabolites along the glycolytic cascade (fig. S13A). Inhibition of glucose metabolism via 2-deoxyglucose (2-DG) rescued glucose-induced barrier aberrations in vitro in a dose-dependent manner (Fig. 5, A to C). In addition, 2-DG administration blocked transcriptional reprogramming in STZ-treated mice (Fig. 5D and fig. S13B), including the N-glycan pathway (fig. S13C); prevented the systemic dissemination of microbial products (Fig. 5, E and F); and restored host defense against *C. rodentium* (Fig. 5G and fig. S13, D to F). Bacterial growth in the intestinal lumen was unaffected by 2-DG treatment (fig. S13G). To test whether 2-DG could be used to counteract hyperglycemia-mediated loss of barrier integrity beyond the STZ model, we administered 2-DG to *C. rodentium*-infected *db/db* mice and assessed its impact on systemic dissemination of the pathogen. Notably, the detectable pathogen load in the mesenteric lymph nodes, spleens, and livers of 2-DG–treated *db/db* mice was strongly reduced under 2-DG treatment (Fig. 5H and fig. S13, H and I). Together, these data suggest that glucose-mediated reprogramming of epithelial cell metabolic function leads to transcriptional alterations, abrogation of the intestinal barrier, and impaired host defense against enteric infection.

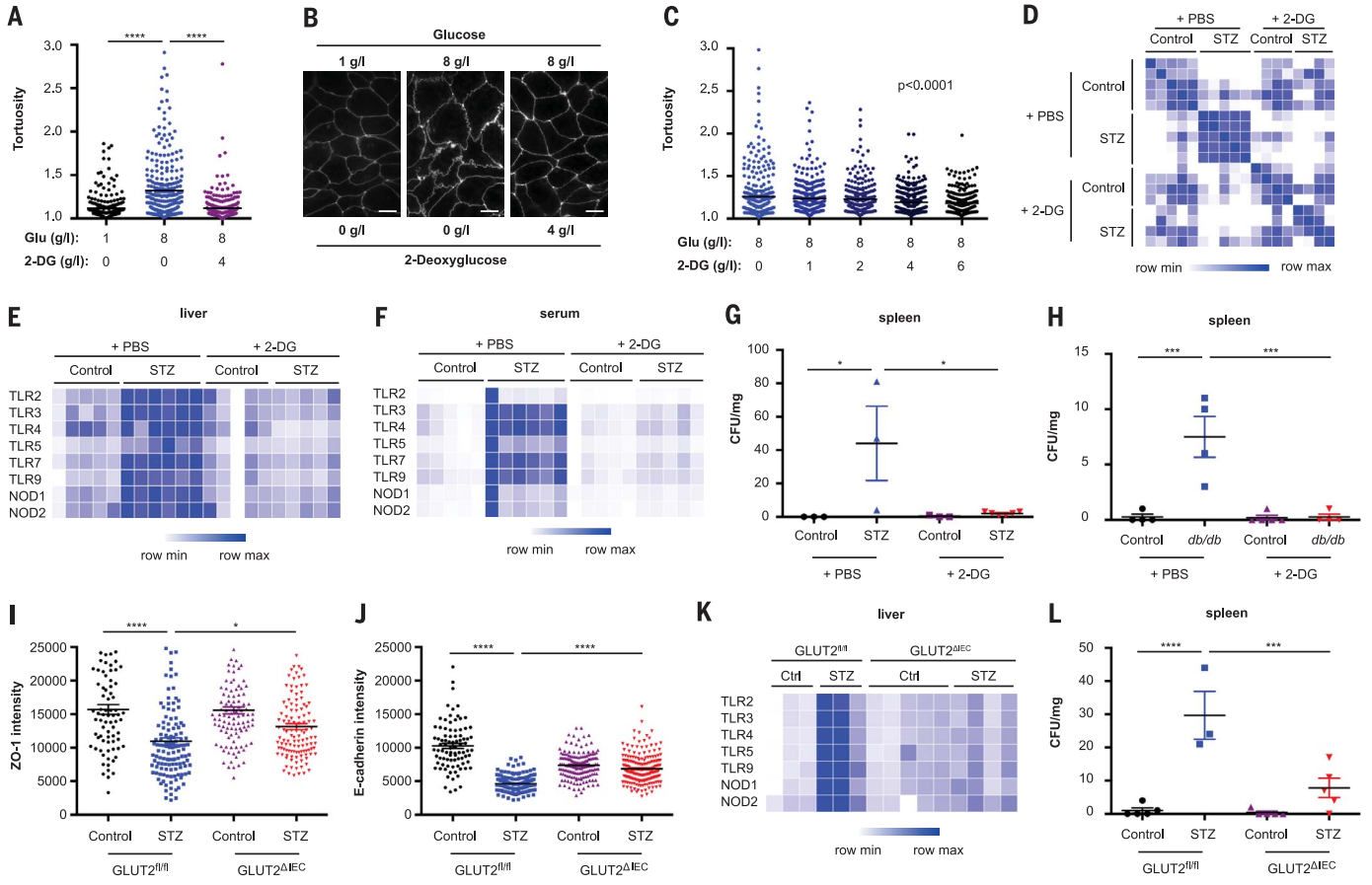

Fig. 5. Epithelial reprogramming by hyperglycemia involves glucose metabolism and GLUT2. (**A** to **C**) Quantification of barrier tortuosity (A and C) and representative ZO-1 staining (B) of Caco-2 cells treated with the indicated concentrations of glucose and 2-deoxyglucose (2-DG). Scale bars, 10 μm. (**D**) Similarity matrix of the epithelial transcriptomes of STZ-treated mice, with or without 2-DG administration. (**E** and **F**) PRR stimulation by hepatic extracts (E) and sera (F) from STZ-treated mice, with or without 2-DG administration. (**G** and **H**) Splenic CFUs from *C. rodentium*–infected and 2-DG–treated STZ (G) and *db/db* mice (H). (**I** to **K**) Colonic ZO-1 (I) and E-cadherin intensity (J) and PRR stimulation by hepatic extracts (K) from STZ-treated GLUT2$^{\Delta IEC}$ mice and controls. (**L**) CFUs recovered from spleens of STZ-treated GLUT2$^{\Delta IEC}$ mice and controls infected with *C. rodentium*. All data represent at least two independent experiments. Means ± SEM are plotted. $^{*}P < 0.05$, $^{**}P < 0.01$, $^{***}P < 0.001$, $^{****}P < 0.0001$ by ANOVA.

Glucose transport between the intestinal epithelium and circulation is mediated by the bidirectional glucose transporter GLUT2 (*31*). To determine the role of this transporter in hyperglycemia-mediated epithelial reprogramming, we next used mice selectively lacking GLUT2 in intestinal epithelial cells (GLUT2$^{\Delta IEC}$) (*32*) and induced hyperglycemia in these mice by STZ administration. Indeed, GLUT2$^{\Delta IEC}$ mice were resistant to STZ-induced transcriptional reprogramming and retained epithelial transcriptomes similar to those of controls (fig. S14, A and B). GLUT2$^{\Delta IEC}$ mice also retained intact tight and adherence junction complexes (Fig. 5, I and J, and fig. S14, C and D), reduced transepithelial flux (fig. S14E), and intestinal containment of microbial PRR ligands (Fig. 5K), despite sustained STZ-induced hyperglycemia (fig. S14F). Ablation of GLUT2 also ameliorated the STZ-induced susceptibility to *C. rodentium* growth and systemic dissemination (Fig. 5 L, and fig. S14, G to I). Collectively, these results indicate that GLUT2 is involved in the hyperglycemia-induced metabolic and transcriptional alterations in intestinal epithelial cells, resulting in barrier dysfunction and microbial translocation to the systemic circulation.

Blood glucose concentrations are associated with microbial product influx in humans

Finally, we sought to determine whether glycemic levels similarly correlate with intestinal barrier function in humans. To this end, we recruited 27 healthy individuals (fig. S15, A and B) and performed measurements of multiple serum parameters and microbial products in the circulation. Of all variables measured, hemoglobin A1c (HbA1c), indicative of an individual's 3-month average plasma glucose concentration, showed the strongest correlation with serum levels of PRR ligands (Fig. 6, A to C, and fig. S15, C to E). In contrast, high body mass index and other hallmarks of metabolic disease did not significantly associate with the influx of microbial products (Fig. 6, A and B, and fig. S15F). Total stool bacterial content did not correlate with HbA1c levels (fig. S15G). Together, these data suggest that similar to their effects in mice, serum glucose concentrations, rather than obesity, may associate with or potentially even drive intestinal barrier dysfunction in humans.

Discussion

Serum glucose is among the most strictly controlled physiological variables of organismal homeostasis. Chronically elevated glucose concentrations, as observed in diabetes mellitus, obesity, and associated metabolic disorders, such as nonalcoholic fatty liver disease, result from altered homeostatic set points of the tightly regulated normoglycemic levels (*33*). Long-standing hyperglycemia, in turn, leads to a myriad of potentially devastating biochemical and physiological consequences, such as the generation of advanced glycation end products, pancreatic glucose toxicity (*34*, *35*), macrovascular and microvascular complications affecting virtually every organ (*36*), risk of infection (*37*), and enhanced mortality (*38*).

In this study, we have identified glucose as an orchestrator of intestinal barrier function. Hyperglycemia markedly interfered with homeostatic epithelial integrity, leading to abnormal influx of

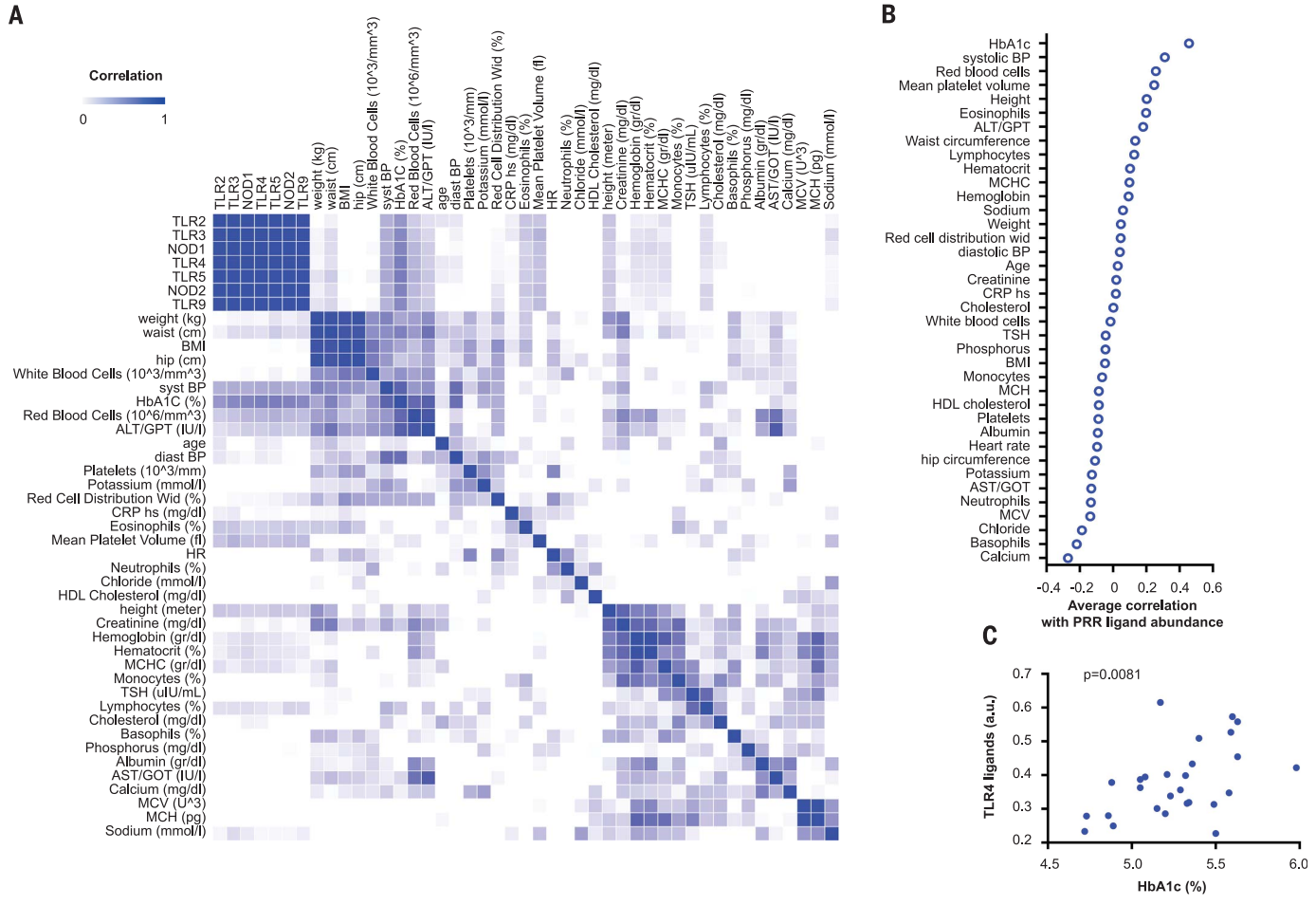

Fig. 6. Hyperglycemia is associated with influx of microbial products in humans. (**A** and **B**) Correlation matrix (A) and average correlations with systemic PRR ligands (B) of the indicated parameters in the serum of 27 healthy volunteers. (**C**) Correlation of HbA1c with serum levels of TLR4 ligands.

immune-stimulatory microbial products and a propensity for systemic spread of enteric pathogens. Our results indicate that hyperglycemia causes retrograde transport of glucose into intestinal epithelial cells via GLUT2, followed by alterations in intracellular glucose metabolism and transcriptional reprogramming (fig. S16). One of the most strongly affected pathways by hyperglycemia in our study involves the N-glycosylation of proteins in the endoplasmic reticulum and Golgi apparatus, which has been implicated as a key regulator of a multitude of epithelial functions (*25*). Although our study focused on the impact of systemic glucose concentrations on the intestinal barrier, similar effects might be caused by a high-glucose diet, which may affect intestinal epithelial cells in a similar manner, potentially resulting in diet-induced alterations of barrier function. Such potential physiologically important dietary effects on barrier function merit further studies. Furthermore, the impact of hyperglycemia on epithelial barrier function might be relevant beyond the gastrointestinal tract and affect other mucosal surfaces, such as the respiratory tract, as was indicated by a recent study of close to 70,000 diabetes patients highlighting a positive correlation between HbA1c values and a variety of mucosal community- and hospital-acquired infections (*39*).

Collectively, our findings provide a potential molecular explanation for altered barrier function in the context of the metabolic syndrome and the resultant enhanced mucosal infection noted in patients suffering from obesity (*5*) and diabetes mellitus (*40*). Furthermore, the link that we highlight between hyperglycemia and gut barrier alterations may provide a mechanistic basis for a variety of seemingly unrelated inflammatory manifestations, complications, and associations of the metabolic syndrome—collectively termed "metaflammation" or "para-inflammation" (*41*, *42*). Examples of these include adipose tissue inflammation driving exacerbated obesity and glucose intolerance (*43*), nonalcoholic fatty liver disease progressing to detrimental nonalcoholic steatohepatitis (*44*), inflammation contributing to atherosclerosis and associated cardiovascular disease (*45*), and even recently suggested associations between the metabolic syndrome and neurodegeneration (*46*). Ultimately, our results may present the starting point for harnessing glucose metabolism or other regulators of intestinal barrier integrity as potential therapeutic targets in the prevention and amelioration of enteric infection and gut-related systemic inflammation.

REFERENCES AND NOTES

1. N. Stefan, F. Schick, H. U. Häring, *Cell Metab.* **26**, 292–300 (2017).
2. D. A. Winer, H. Luck, S. Tsai, S. Winer, *Cell Metab.* **23**, 413–426 (2016).
3. P. D. Cani *et al.*, *Diabetes* **57**, 1470–1481 (2008).
4. M. E. Falagas, M. Kompoti, *Lancet Infect. Dis.* **6**, 438–446 (2006).
5. K. A. Kaspersen *et al.*, *Epidemiology* **26**, 580–589 (2015).
6. J. Casqueiro, J. Casqueiro, C. Alves, *Indian J. Endocrinol. Metab.* **16** (suppl. S1), 27–36 (2012).
7. S. I. Grivennikov *et al.*, *Nature* **491**, 254–258 (2012).
8. T. R. Sampson *et al.*, *Cell* **167**, 1469–1480.e12 (2016).
9. N. Thevaranjan *et al.*, *Cell Host Microbe* **21**, 455–466.e4 (2017).
10. R. Ahmad, B. Rah, D. Bastola, P. Dhawan, A. B. Singh, *Sci. Rep.* **7**, 5125 (2017).
11. N. M. Mackey-Lawrence, W. A. Petri Jr., *Mucosal Immunol.* **5**, 472–479 (2012).
12. X. Wang *et al.*, *Nature* **514**, 237–241 (2014).
13. R. Madan *et al.*, *Infect. Immun.* **82**, 341–349 (2014).
14. C. Guillot, T. Lecuit, *Science* **340**, 1185–1189 (2013).
15. J. W. Collins *et al.*, *Nat. Rev. Microbiol.* **12**, 612–623 (2014).
16. M. Wlodarska *et al.*, *Cell* **156**, 1045–1059 (2014).
17. M. G. Myers Jr., H. Münzberg, G. M. Leinninger, R. L. Leshan, *Cell Metab.* **9**, 117–123 (2009).
18. E. Elinav *et al.*, *Endocrinology* **150**, 3083–3091 (2009).
19. M. S. Islam, D. T. Loots, *Methods Find. Exp. Clin. Pharmacol.* **31**, 249–261 (2009).
20. J. Wang *et al.*, *J. Clin. Invest.* **103**, 27–37 (1999).
21. D. W. Scott *et al.*, *Mol. Biol. Cell* **26**, 3205–3214 (2015).
22. M. Nita-Lazar, I. Rebustini, J. Walker, M. A. Kukuruzinska, *Exp. Cell Res.* **316**, 1871–1884 (2010).

23. B. T. Jamal *et al.*, *Cell Health Cytoskelet.* **2009**, 67–80 (2009).
24. Y. Goto *et al.*, *Science* **345**, 1254009 (2014).
25. Y. Goto, S. Uematsu, H. Kiyono, *Nat. Immunol.* **17**, 1244–1251 (2016).
26. T. A. Pham *et al.*, *Cell Host Microbe* **16**, 504–516 (2014).
27. J. M. Pickard *et al.*, *Nature* **514**, 638–641 (2014).
28. K. S. Bergstrom *et al.*, *PLOS Pathog.* **6**, e1000902 (2010).
29. M. Van der Sluis *et al.*, *Gastroenterology* **131**, 117–129 (2006).
30. S. Niu *et al.*, *J. Immunol.* **197**, 3293–3301 (2016).
31. B. Thorens, *Diabetologia* **58**, 221–232 (2015).
32. C. C. Schmitt *et al.*, *Mol. Metab.* **6**, 61–72 (2016).
33. M. E. Kotas, R. Medzhitov, *Cell* **160**, 816–827 (2015).
34. A. Bangert *et al.*, *Proc. Natl. Acad. Sci. U.S.A.* **113**, E155–E164 (2016).
35. Y. Tanaka, P. O. Tran, J. Harmon, R. P. Robertson, *Proc. Natl. Acad. Sci. U.S.A.* **99**, 12363–12368 (2002).
36. R. Madonna, R. De Caterina, *Vascul. Pharmacol.* **54**, 68–74 (2011).
37. S. O. Butler, I. F. Btaiche, C. Alaniz, *Pharmacotherapy* **25**, 963–976 (2005).
38. S. A. Leite *et al.*, *Diabetol. Metab. Syndr.* **2**, 49 (2010).
39. A. Mor *et al.*, *Am. J. Epidemiol.* **186**, 227–236 (2017).
40. L. M. Muller *et al.*, *Clin. Infect Dis.* **41**, 281–288 (2005).
41. R. Medzhitov, *Nature* **454**, 428–435 (2008).
42. G. S. Hotamisligil, *Nature* **542**, 177–185 (2017).
43. D. Okin, R. Medzhitov, *Cell* **165**, 343–356 (2016).
44. A. Nakamura *et al.*, *J. Diabetes Investig.* **2**, 483–489 (2011).
45. F. Pistrosch, A. Natali, M. Hanefeld, *Diabetes Care* **34** (suppl. 2), S128–S131 (2011).
46. M. Barbagallo, L. J. Dominguez, *World J. Diabetes* **5**, 889–893 (2014).

ACKNOWLEDGMENTS

We thank the members of the Elinav lab for discussions, J. Friedman for providing mice, and A. Erez and S. Limanovich for helpful advice. **Funding:** C.A.T. received a Boehringer Ingelheim Fonds PhD Fellowship. B.G. holds the Erwin Neter professorial Chair in cell and tumor biology. B.G. and E.E. are supported by the Leona M. and Harry B. Helmsley Charitable Trust; E.E. is supported by Y. and R. Ungar; the Adelis Foundation; the Gurwin Family Fund for Scientific Research; the Crown Endowment Fund for Immunological Research; the estate of J. Gitlitz; the estate of L. Hershkovich; the Benoziyo Endowment Fund for the Advancement of Science; J. L. and V. Schwartz; A. and G. Markovitz; A. and C. Adelson; the French National Center for Scientific Research (CNRS); D. L. Schwarz; the V. R. Schwartz Research Fellow Chair; L. Steinberg; J. N. Halpern; A. Edelheit; and by grants funded by the European Research Council; a Marie Curie Integration grant; the German-Israeli Foundation for Scientific Research and Development; the Israel Science Foundation; the Helmholtz Foundation; and the European Foundation for the Study of Diabetes. P.S. and A.G. acknowledge ANR-ALIA 007-01 Nutra2-sense for the generation of the intestinal epithelial-specific GLUT2 knockout mice. E.E. holds the Sir Marc & Lady Tania Feldmann professorial Chair in immunology, is a senior fellow of the Canadian Institute for Advanced Research (CIFAR), and an international researcher of the Bill & Melinda Gates Foundation and Howard Hughes Medical Institute (HHMI). **Author contributions:** C.A.T. conceived the study; designed, performed, analyzed, and interpreted experiments; and wrote the manuscript. M.L., I.G., D.Z., E.S., E.B., S.B., A.C.T., M.N.K. and M.P.-F. performed and analyzed experiments. O.B., M.E., R.B.-Z., D.L-R., Z.H., and S.A. carried out the human study. A.G., A.H., P.S., A.G., H.G., and B.G. provided critical tools, insights, and advice. E.E. conceived the study, supervised and mentored its participants, interpreted results, and wrote the manuscript. **Competing interests:** The authors declare that they have no competing interests. **Data and materials availability:** All data and code to understand and assess the conclusions of this research are available in the main text, supplementary materials, and via the following repositories: European Nucleotide Archive (ENA) accession no. PRJEB24760.

SUPPLEMENTARY MATERIALS

www.sciencemag.org/content/359/6382/1376/suppl/DC1
Materials and Methods
Figs. S1 to S16
References (*47–56*)

26 October 2017; accepted 6 February 2018
Published online 8 March 2018
10.1126/science.aar3318

Hyperglycemia drives intestinal barrier dysfunction and risk for enteric infection

Christoph A. Thaiss, Maayan Levy, Inna Grosheva, Danping Zheng, Eliran Soffer, Eran Blacher, Sofia Braverman, Anouk C. Tengeler, Oren Barak, Maya Elazar, Rotem Ben-Zeev, Dana Lehavi-Regev, Meirav N. Katz, Meirav Pevsner-Fischer, Arieh Gertler, Zamir Halpern, Alon Harmelin, Suhail Aamar, Patricia Serradas, Alexandra Grosfeld, Hagit Shapiro, Benjamin Geiger and Eran Elinav

Science **359** (6382), 1376-1383.
DOI: 10.1126/science.aar3318originally published online March 8, 2018

Metabolic syndrome, leaky guts, and infection

Metabolic syndrome often accompanies obesity and hyperglycemia and is associated with a breakdown in the integrity of the intestinal barrier and increased risk of systemic infection. Thaiss *et al.* found that mice with systemic infection of a *Salmonella* analog, *Citrobacter rodentium*, also exhibited hyperglycemia. Deletion of the glucose transporter GLUT2 altered sensitivity to chemically induced epithelial permeability and protected mice from pathogen invasion. The authors also found a correlation in humans between glycated hemoglobin (an indicator of hyperglycemia) and serum levels of pathogen recognition receptor ligands.

Science, this issue p. 1376